Available online at www.sciencedirect.com
SCIENCE DIRECT®
Microelectronic Engineering 75 (2004) 24–30
MICROELECTRONIC ENGINEERING
www.elsevier.com/locate/mee

Quantitative characterization of electromigration-induced plastic deformation in Al(0.5wt%Cu) interconnect

R.I. Barabash [a,*], G.E. Ice [a], N. Tamura [b], B.C. Valek [c], J.C. Bravman [c], R. Spolenak [d], J.R. Patel [b,e]

[a] *Metals and Ceramics Division, Oak Ridge National Laboratory, Oak Ridge, TN 37831, USA*
[b] *Advanced Light Source, 1 Cyclotron Road, Berkeley, CA 94720, USA*
[c] *Department of Materials Science and Engineering, Stanford University, Stanford, CA 94305, USA*
[d] *Max Planck Institut für Metallforschung, Heisenbergstrasse 3, D-7056 Stuttgart, Germany*
[e] *Stanford Synchrotron Radiation Laboratories, P.O. BOX 4349, Stanford, CA 94309, USA*

Received 14 July 2003; received in revised form 28 July 2003; accepted 10 September 2003
Available online 26 February 2004

Abstract

Electromigration-induced failure in metal interconnect constitutes a major reliability problem in the semiconductor industry. Recently, experimental techniques capable of probing grain orientation and stress with a spatial resolution compatible with the dimensions of the lines have emerged. White beam X-ray microdiffraction is particularly well suited to the in situ study of electromigration. The technique was used to probe microstructure in interconnects and recently unambiguously unveiled the plastic nature of the deformation induced by mass transport during electromigration in Al(Cu) interconnect lines even before macroscopic damage. The aim of the present research is to understand the complex dislocation structure arising from electromigration-induced plastic deformation by simulating the shape of the reflections and comparing them with the shape observed in the experimental data. We provide a first quantitative analysis of the dislocation structure generated in individual micron-sized Al grains during an in situ electromigration experiment. Custom software allows us to determine the orientation of the predominant dislocation network in each sample subgrain.

Keywords: Electromigration; Dislocations; Interconnects; Diffraction; Characterization

1. Introduction

The decrease of interconnect line dimensions with a simultaneous increase in current density to 1 mA/cm^2 has imposed tremendous challenges for materials and reliability of interconnects. Electromigration depletes material at the cathode end of the interconnect line and causes accumulation near the anode end [1]. Electromigration-induced failure in metal interconnect constitutes a major reliability problem in the semiconductor industry [2]. While the general mechanism of

* Corresponding author. Tel. +865-2417230; fax: +865-5747659.
E-mail address: barabashr@ornl.gov (R.I. Barabash).

0167-9317/$ - see front matter © 2004 Elsevier B.V. All rights reserved.
doi:10.1016/j.mee.2003.09.009

electromigration is understood [3], the effect of the atomic flow on the local metallic line microstructure is largely unknown. White beam X-ray microdiffraction [4–14] was used to probe microstructure in interconnects [4,11–14] and has recently unambiguously unveiled the plastic nature of the deformation induced by mass transport during electromigration in Al(Cu) lines [15] even before macroscopic damage occurs. The first quantitative analysis of dislocation structure in a grain in the polycrystalline region of the interconnect line was performed in [16,17] and it was shown that in that region of the interconnect line the dislocations which have their lines almost parallel to the current flow direction are formed first. Recent study of precipitation in Al(Cu) interconnects [18] indicates that Cu is preferentially depleted from the cathode end of the line. Analysis of alloying effects in electromigration [19] demonstrates our incomplete understanding of why the addition of Cu results in a great improvement of electromigration resistance of Al-based interconnect lines.

The aim of the present paper is to understand the complex dislocation structure arising from electromigration-induced plastic deformation in different regions (including the ends) of interconnect lines and to find the possible correlation between Cu drift, precipitation and formation of dislocations.

2. Experimental

Data collection has been carried out at the X-ray microdiffraction end station on beamline 7.3.3 at the Advanced Light Source. The sample is a patterned Al(0.5wt%Cu) line (length: 30 μm, width 4.1 μm, thickness 0.75 μm) sputter deposited on a Si wafer and buried under a glass passivation layer (0.7 μm thick). Electrical connections to the line are made through unpassivated Al(Cu) pads connected to the sample through W vias. In the present paper, we concentrate on the evolution of the diffraction pattern of four particular grains (grains A–E, size: ~2.5 μm situated approximately at the middle of the line, and grains F and G close to the opposite ends of the line). Details on the experimental setting and data collection can be found elsewhere [4–6]. A qualitative description and semi-quantitative interpretation of the entire data set collected for the present sample can be found in a recent article [15]. Orientation maps obtained from the X-ray microdiffraction scans reveal that the grain structure of the line has a pronounced (1 1 1) fiber texture. Only one or a few grains span the width of the line (near a bamboo configuration). Grains A and E are in a region of the line where multiple grains are found transverse to the line, and grains F and G are almost at the ends of the line. Dislocation structure was determined from the Laue images by simulating the shape of the reflections observed in the experimental data. Custom software allows us to determine the orientation of the predominant dislocation network in each sample subgrain [16,17,20]. Here we extended this method to consider gradients with depth in the number of randomly distributed geometrically necessary dislocations (GNDs). We assume that scattering domains are separated by geometrically necessary dislocation boundaries (GNBs). We also determine the strain gradient parameters with white beam diffraction.

3. Results and discussion

Before electromigration all Laue patterns show sharp reflections for all grains (spot 1 in Fig. 1(a–d)), and pronounced streaking of the Laue reflections from all Al grains after electric current flow (Fig. 1(a–d) (spot 5). The average streaking direction for the grains in the middle of the line is approximately transverse to the length of the line (Fig. 1(a) and (b)). (Note: this is generally true for the majority of the grains in the lines except a few of them at the ends.) Streaking is almost parallel to the line near the end (Fig. 1(c) and (d)). During the first 16 h of migration, grain F is close to the anode (Fig. 1(c), spots 1–3), which becomes the cathode after current reversal (Fig. 1(c), spots 4 and 5), and grain G is in the opposite end of the interconnect line.

The Laue spot intensity profiles along the streak at different times during the electromigration

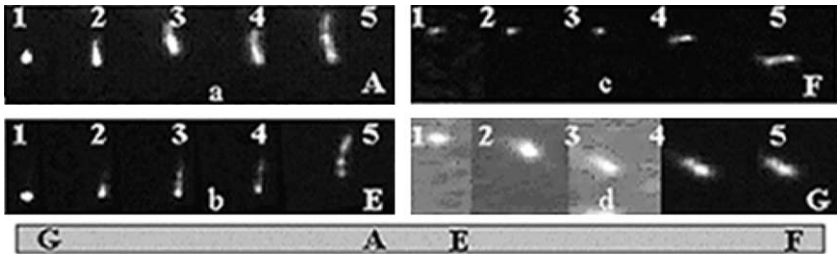

Fig. 1. Change of experimental streaking of (2 2 2) Laue spots for grains A and E in the middle of the line (a, b) and for grains F and G (c, d) close to the opposite ends of the interconnect line. The sample was maintained at a constant temperature of 205 °C (1) and the current density was progressively ramped up to $J = 0.98$ mA/cm^2, and maintained at this value for up to 16 h (2, 3). The direction of the current was then reversed for a total period of 19 h: (1) initial state before the current flow; (2) 5 h; (3) 16 h; (4) 9 h reversed current; (5) 19 h reversed current.

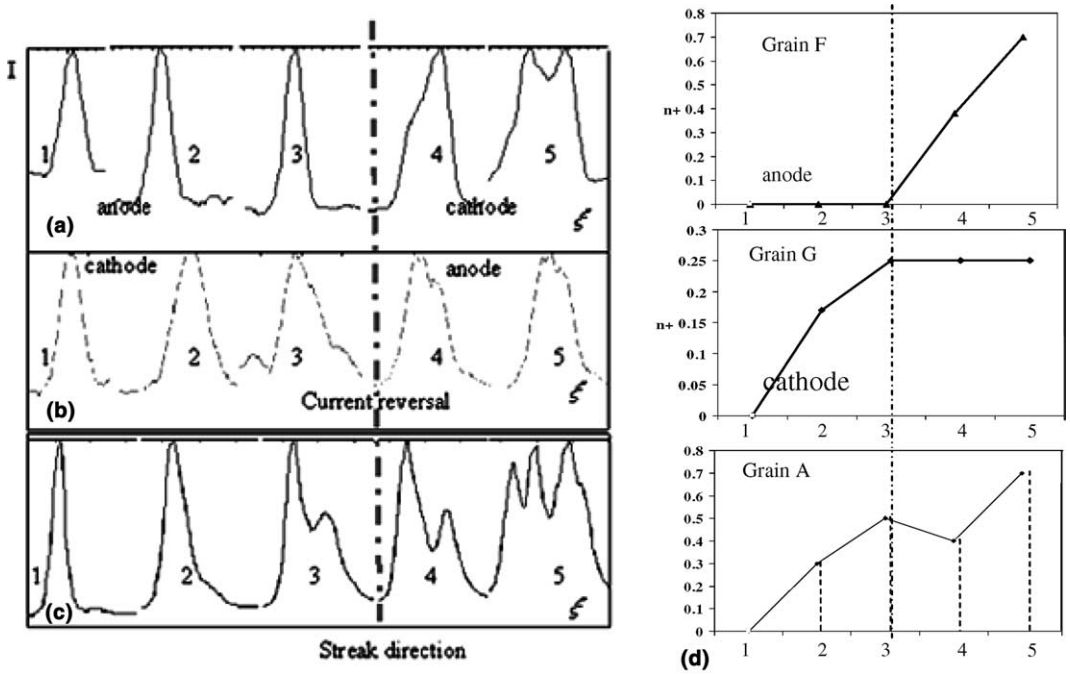

Fig. 2. Intensity distribution I (in arbitrary units) along the streak direction (in pixel) for grains F (a), G (b) located near the opposite ends of the interconnect line and grain E (c) in the middle of the interconnect line with time of current flow: (1) initial state before the current flow; (2)5 h; (3)16 h; (4) 9 h reversed current; (5) 19 h reversed current; Dislocation density n^+ (in 10^{10} cm^{-2}) with time of electromigration in the grains A, G, and F (d).

process are presented in Fig. 2 for grains F, G and E in reciprocal space in sample basis. For the grain labeled E (in the middle of the line) continuous streaks are observed near all Laue spots in the measurements made after 5 h of electromigration at $J = 0.98$ mA/cm^2. Although the in-plane orientation of grain E differs from grain A, the evolution of Laue spots with time of current flow is similar to the one observed for grain A [15–17]. After 16 h of current flow, the (2 2 2) Laue spot becomes a streak with strong intensity maximum on one side and a long weak tail.

It was recently shown that streaking and splitting of Laue images can be used to determine the

orientation and density of the activated dislocation network [16,17,20]. The direction of the long axes of the streak ξ and the full width at half maximum (FWHM_{ξ}) in the long direction of the streak depend on the total number of unpaired GNDs along the beam, their mutual orientation with the Laue spot momentum transfer G_{hkl}, and the incident X-ray beam direction.

As a result of dislocation motion and the strong interaction between dislocations, a random dislocation distribution becomes unstable and forms a correlated dislocation arrangement into dislocation walls. Some fraction of the dislocations may remain randomly distributed. As dislocations are removed from the fragments and added to the dislocation walls, a *correlated* misorientation develops between the neighboring parts of the crystal. When the dislocation walls are well developed, so that the distance h between dislocations within the wall is much shorter than the distance between the walls D ($h \ll D$), the intensity distribution becomes discontinuous. Such walls produce sharp rotations of the crystal fragments with an abrupt rotational phase variation.

To determine the amount of boundary dislocations, we define the average distance D between the two neighboring GNBs. We write the number of such dislocation walls per unit length as $1/D$. The total density of unpaired dislocations grouped in the walls, n, is defined by

$$n^{\mathrm{w}} = \frac{1}{Dh}. \tag{1}$$

The mean deformation tensor ω^{w} due to the presence of GNBs results in pure rotations about the direction of dislocation lines in the wall. The misorientation angle Θ due to such a boundary is defined by the equation

$$b/h = 2\sin(\Theta/2). \tag{2}$$

Here $b/h \approx \Theta$ for small angle boundaries. For tilt GNB formed by edge dislocations with the Burgers vector **b** parallel to the X axis but perpendicular to the slip plane normal $\boldsymbol{N}$, the two non-zero components of the mean deformation tensor, ω^{w}_{xN} and ω^{w}_{Nx}, are equal

$$\omega^{\mathrm{w}}_{xN} = -\omega^{\mathrm{w}} Nx = \Theta x/D. \tag{3}$$

If the angular misorientation between GNBs is sufficiently large, the reflection becomes discontinuous. To understand this dependence, we assume that along the penetration depth L, the X-ray beam intersects several fragments with average size D. Each fragment contributes to the diffraction. The number of such contributions is L/D. Each boundary produces an average misorientation Θ. The average distance between the Laue maximums, Δ, formed by two adjacent fragments is $\Delta = \frac{G_{hkl}}{k_0}\Theta$. Here k_0 is the incident wave vector corresponding to the energy of the X-rays for the (hkl) Laue spot. If this distance Δ exceeds the average FWHM of the Laue image for each fragment along the ξ axis, the Laue spots splits. Such splitting is observed at Laue spots for grains A and E after 19 h of electromigration (Fig. 1). This gives us the possibility to measure the misorientation angle Θ thorough the boundary. Using the approach [16,17] and Eqs. (1)–(3), we determine the orientation and density of random and boundary dislocations.

The orientation of the primary GNDs in the grain E corresponds to a Burgers vector $bfb = [\bar{1}\,1\,0]$ and a dislocation line, $\tau = [1\,1\,\bar{2}]$, and is almost parallel to the direction of the current flow in that grain. After 11 h at the same current density, the intensity distribution in grains E breaks into two distinct maxima (Fig. 2(c), curve 3) indicating that the dislocation structure partially relaxed with the formation of a GNB. The density of boundary dislocations is about 0.25×10^{10} cm^{-2}. The FWHM_{ξ} along the streak direction ξ within each maximum also increased (Fig. 2(c), curve 3). The density of unpaired individual dislocations within each scattering domain at this stage is equal to $n^{+} = 0.3 \times 10^{10}$ cm^{-2} (Fig. 2(c)). We then reversed the direction of the current flow to $J = -0.98$ mA/cm^2. After 9 h the randomly distributed dislocation population decreases, while the portion of dislocations grouping within the GNB increased (Fig. 2(c), curve 4). This indicates that the opposite direction of the current may actually reverse some part of the randomly distributed unpaired individual dislocations. The density of unpaired individual dislocations within each scattering domain slightly decreased from $n^{+} = 0.3 \times 10^{10}$ to 0.2×10^{10} cm^{-2}. However, the

dislocations being grouped into a sub-boundary form a very stable arrangement, which is not destroyed by the current in the opposite direction. After 10 h with $J = -0.98$ mA/cm^2, a second sub-boundary is formed. The streak splits into three distinct maximums (Fig. 2(c), curve 5). The second geometrically necessary boundary creates misorientation of 0.4^0. The total density of boundary dislocations within the above two boundaries is equal to 0.6×10^{10} cm^{-2}. It should be noted that the orientation of the secondary slip system in both grain A and E is slightly inclined to the direction of the current flow.

Our analysis of the orientation of the activated dislocation slip systems shows that in the polycrystalline region in the middle of the interconnect line the slip systems with dislocation lines almost parallel to the direction of current flow are activated first.

Grains F and G (Figs. 1(c), (d) and 2(a), (b)) in the opposite ends of the interconnect line show a distinct behavior compared to the grains A and E in the middle of the line. Grain F in the beginning of the experiment is close to the anode end of the line. There is absolutely no increase in the FWHM$_\xi$, which indicates the absence of plastic deformation in this grain during this period of current flow (moreover the FWHM in all directions of the spot slightly decrease). After the current reversal, the grain F becomes close to the cathode end of the line and its FWHM$_\xi$, along the streak direction immediately increases, indicating a highly active plastic deformation. The density of geometrically necessary dislocations becomes $n^+ = 0.3 \times 10^{10}$ cm^{-2}. The orientation of the primary GNDs corresponds to a Burgers vector $\mathbf{b} = [\bar{1}\,0\,1]$ and a dislocation line direction $\tau = [1\,\bar{2}\,1]$ (Fig. 3 left side) and is almost perpendicular to the direction of the current flow. The next 10 h of the current flow in the same direction result in the grouping of dislocations within a GNB. Grain G demonstrates the opposite behavior (Figs. 1(d) and 2(b)).

Immediately after the current is on grain *G* (located close to the cathode end of the line) shows the increase in the FWHM$_\xi$ of the Laue streak. Just opposite to grains E and F, the (2 2 2) Laue spot in grain G first broadens symmetrically (Fig. 2(b), curve 2). After 6 additional hours at the same current density, the intensity distribution becomes highly asymmetric (with intensity maximum on one side of the streak followed by a long tail of decreasing intensity) and corresponds to a dislocation density of $n^+ = 0.4 \times 10^{10}$ cm^{-2} (Fig. 2(b), curve 3). After current reversal, the FWHM$_\xi$, of the streak slightly decreases, and the intensity distribution breaks into two distinct maxima (Fig. 2(b), curve 4) indicating that the dislocation structure partially relaxed with the formation of a GNB. The continuation of the current flow in this direction (with

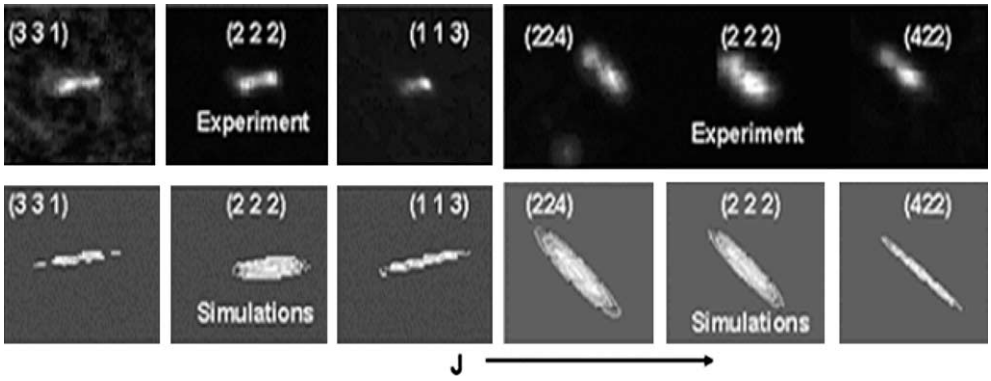

Fig. 3. Experimental (top) and simulated (bottom) stereographic projections of different Laue streaks for grains F (left) and G (right). Simulations were performed for activated slip systems with Burgers vector $\mathbf{b} = [\bar{1}\,0\,1]$ and a dislocation line direction $\tau = [1\,\bar{2}\,1]$ for F grain, and for two activated slip systems with $\mathbf{b} = [0\,1\,1]$ and dislocation lines in directions $\tau_1 = [\bar{2}\,\bar{1}\,1]$ and $\tau_2 = [2\,\bar{1}\,1]$ for a G grain. Direction of the current **J** is shown with an arrow at the bottom of the figure.

grain G remaining close to the anode end of the line) does not increase the $FWHM_{\xi}$, *of the streak*. This indicates the absence of dislocation activity in this grain during its position as the "near anode" period of the test.

To determine the orientation of the activated slip systems, we have simulated the Laue streaks corresponding to the activated dislocation arrangements in grains F and G. In Fig. 3, the experimental and simulated (3 3 1), (2 2 2) and (1 1 3) Laue streaks are shown for the grain F (left) and (2 2 4), (2 2 2) and (4 2 2) Laue streaks for grain G (right). Laue streaks are shown in reciprocal space in the sample basis. Although the orientation of streaks is different in different grains, the experimental and simulated streaks remain parallel to each other.

Such peculiarities of plastic deformation in the "near anode/cathode" regions can be understood by taking into account that Cu is preferentially depleted from the cathode region of the interconnect line [18,19]. Moreover, the Al(0.5wt%Cu) interconnect line in the initial state might contain small ($\sim$1.2 nm) precipitates of the tetragonal phase (Al_2Cu) [18]. The dissolution kinetics of this phase near the cathode end is coupled to the plastic deformation activity. During the time of the electromigration test, there is no visible dislocation activity close to the anode end of the line (as observed in this study), while the "near cathode" grain is quickly plastically deformed. Laue diffraction analysis of different grains along the interconnect line shows that the degree of plastic deformation is dependent on the position of the grain within the line [15]. To interpret such a behavior, we expand the model of electromigration-induced Cu motion and precipitation in Al(0.5wt%Cu) interconnects described in [18]. We take into account the coupling between plastic deformation and precipitation formation and dissolution in different regions of the line. Presence of small precipitates is known to strengthen the Al-based alloys and increase their resolved shear stress. Cu depletion in the near cathode region causes dissolution of precipitates. The decrease of precipitates size at first causes symmetric broadening of the Laue spot as observed here (Fig. 2(b), curve 2). After precipitates dissolve, the critical shear stress decreases and plastic deformation is activated. This is accompanied with streaking and further splitting of the Laue spots (Fig. 2(b), curve 3). With the reversal of current flow, Cu concentration in this grain starts to increase and precipitations form again. Critical shear stress increases in this grain and plastic activity stops (Fig. 2(b), curves 4 and 5). The dislocation grouping in the wall is stable and not destroyed by this process. However, new dislocations do not appear. In the "near anode" grain F, an increase of Cu concentration slightly increases the size of the precipitate which slightly decreases the FWHM of the Laue spot (Fig. 1(a), curves 2 and 3). Critical shear stress is high in grain F and plastic activity is suppressed. Reversal of current flow is accompanied with dissolution of precipitates. Critical shear stress decreases and plastic deformation occurs (Fig. 2(a), curves 4 and 5). This supports the idea [18] that Al(0.5wt%Cu) interconnects are most reliable with less failures when Cu depletion from the cathode end is the slowest. Recent findings from the diffraction pattern show dissolution at the cathode end and growth of Al_2Cu precipitates at the anode end in support of this model [22].

It is worth noting that the start of plastic activity in all grains corresponds to a highly anisotropic intensity distribution along the streak with the intensity maximum concentrated on one side of the streak with a long "tail" (Fig. 2(a), curve 4; (b) curve 3; (c) curve 2). Such intensity distribution is related to the gradient of the dislocation density with depth [21]. This supports the model of dislocation climb from the interface into the depth of the interconnect line [16,17,19].

4. Conclusion

Our analysis of the orientation of the activated dislocation slip systems shows that in the polycrystalline region in the middle of the interconnect line the slip systems with dislocation lines almost parallel to the direction of current flow are activated first. Near the ends of the line, plastic activity is coupled with the depletion of Cu from the cathode end of the line. There is practically no plastic activity in the "near anode" end of the line. A gradient of dislocation density into the depth of the interconnect towards the substrate is observed.

We demonstrate coupling between the density of GNDs and the Cu depletion from the cathode. Our model is consistent with the dissolution and growth of Al_2Cu precipitates on opposite ends during electromigration. This is the first time that these effects have been observed.

Acknowledgements

Research is supported by the Director, Office of Science, Office of Basic Energy Sciences, US Department of Energy, under Contract DE-AC05-00OR22725 with UT-Battelle, LLC at Oak Ridge National laboratory and with the Advanced Light Source, Materials Science Division, under the Contract No. DE-AC03-76SF00098 at Lawrence Berkeley National Laboratory.

References

[1] I.A. Blech, J. Appl. Phys. 47 (1976) 1203.
[2] C.V. Thompson, J.R. Lloyd, Mater. Res. Soc. Bull. 18 (1993) 19.
[3] M.A. Korhonen, P. Borgesen, K.N. Tu, C.-Y. Li, J. Appl. Phys. 73 (1993) 3790.
[4] N. Tamura, A.A. MacDowell, R.S. Celestre, H.A. Padmore, B.C. Valek, J.C. Bravman, R. Spolenak, W.L. Brown, T. Marieb, H. Fujimoto, B.W. Batterman, J.R. Patel, Appl. Phys. Lett. 80 (2002) 3724.
[5] N. Tamura, R. Spolenak, B.C. Valek, A. Manceau, M. Meier Chang, R.S. Celestre, A.A. MacDowell, H.A. Padmore, J.R. Patel, Rev. Sci. Instrum. 73 (2002) 1369.
[6] A.A. MacDowell, R.S. Celestre, N. Tamura, R. Spolenak, B.C. Valek, W.L. Brown, J.C. Bravman, H.A. Padmore, B.W. Batterman, J.R. Patel, Nucl. Instrum. Meth. A 467–468 (2001) 936.
[7] G.E. Ice, B.C. Larson, Adv. Eng. Mater. 2 (10) (2002) 643–646.
[8] B.C. Larson, Wenge Yang, G.E. Ice, J.D. Budai, J.Z. Tischler, Nature 415 (2002) 887–890.
[9] P.-C. Wang, I.C. Noyan, S.K. Kaldor, J.L. Jordan-Sweet, E.G. Liniger, C.-H. Ku, Appl. Phys. Lett. 78 (2001) 2712.
[10] P.C. Wang, G.S. Cargill III, I.C. Noyan, C.K. Hu, Appl. Phys. Lett. 72 (1998) 1296.
[11] N. Tamura, J.-S. Chung, G.E. Ice, B.C. Larson, J.D. Budai, J.Z. Tischler, M. Yoon, E.L. Williams, W.P. Lowe, Mater. Res. Soc. Symp. Proc. 563 (1999) 175.
[12] N. Tamura, B.C. Valek, R. Spolenak, A.A. MacDowell, R.S. Celestre, H.A. Padmore, W.L. Brown, T. Marieb, J.C. Bravman, B.W. Batterman, J.R. Patel, Mat. Res. Soc. Symp. Proc. 612 (2001) D.8.8.1.
[13] R. Spolenak, D.L. Barr, M.E. Gross, K. Evans-Lutherodt, W.L. Brown, N. Tamura, A.A. MacDowell, R.S. Celestre, H.A. Padmore, J.R. Patel, B.C. Valek, J.C. Bravman, P. Flinn, T. Marieb, R.R. Keller, B.W. Batterman, Mat. Res. Soc. Symp. Proc. 612 (2001) D10.3.1.
[14] B.C. Valek, N. Tamura, R. Spolenak, A.A. MacDowell, R.S. Celestre, H.A. Padmore, J.C. Bravman, B.W. Batterman, J.R. Patel, Mat. Res. Soc. Symp. Proc. 673 (2001) P7.7.1.
[15] B.C. Valek, N. Tamura, R. Spolenak, J.C. Bravman, A.A. MacDowell, R.S. Celestre, H.A. Padmore, W.L. Brown, B.W. Batterman, J.R. Patel, Appl. Phys. Lett. 81 (2002) 4168.
[16] R.I. Barabash, G.E. Ice, N. Tamura, B.C. Valek, J.C. Bravman, R. Spolenak, J.R. Patel, J. Appl. Phys. 93 (2003) 5701.
[17] R.I. Barabash, G.E. Ice, N. Tamura, B.C. Valek, J.C. Bravman, R. Spolenak, J.R. Patel, Mat. Res. Soc. 738 (2003), Warrendale Penn.
[18] C. Witt, C. Volkert, E. Arzt, Acta Mater. 51 (2003) 49.
[19] R. Spolenak, O. Kraft, E. Arzt, AIP Conf. Proc. 491 (1999) 126.
[20] R. Barabash, G. Ice, B. Larson, G. Pharr, K. Chung, W. Yang, Appl. Phys. Lett. 79 (2001) 749.
[21] R. Barabash, G.E. Ice, J. Pang, W. Liu, TMS Lett. (2004).
[22] N. Tamura, et al., in press.